International Journal of Multidisciplinary Engineering in Current Research

ISSN NO: 2456 - 4265

Volume 5, Issue 11, November 2020, http://ijmec.com/

Development of a modified Z-source integrated PV/grid/electric vehicle DC charger and inverter

MS J.Nancy Naratha[1], Mrs.T.Sireesha[2], T Naga Bhargavi[3], Addanki Gopinadh[4], Vanigina Narendra[5], G.KrishnaReddy[6]

Assistant Professor[1,2,3,4,5,6]

Department of EEE

NRI INSTITUTE OF TECHNOLOGY, Visadala X Road, Medikonduru(M), Guntur (Dist), Andhra Pradesh 522438.

Abstract:

Based on the sun's rays For residential and semi-commercial uses, energy has been the most common source of sustainable power. Storage structures may be used to mitigate fluctuations in the amount of sunlight-based vitality that can be harvested due to meteorological circumstances. Solar power may also be used to recharge electric car batteries, reducing the need for a network. Such applications need a converter that has fewer alterations organised and provides solitude. Using the Z-source inverter (ZSI) design, many stages are eliminated, allowing for single-stage voltage raise and DC-AC power conversion. Latent sections may also be used to integrate energy storage systems (ESS) into the system. In order to charge the batteries of electric cars (EVs), this study shows how a modified Z-source inverter (MZSI) works in conjunction with a split essential secluded battery charger. The notion of the suggested converter's activity has been shown by reenactment and exploratory results.

Energy storage, photovoltaic (PV) power production, single-phase systems, and transportation electrification are only a few of the topics covered in the index of articles on qZSIs..

I. INTRODUCTION

The use of alternating current power infrastructure is now heavily reliant on charging electric automobiles. Wireless charging and plugging in, even though they are more efficient topologies, may still pollute the environment since they simply use the AC grid. When you know how much fossil fuels are utilised to generate the power required to charge the vehicle, it's much simpler to assess an electric vehicle's carbon impact. One way to reduce carbon footprints is to include renewable energy sources into a charging infrastructure. In order to build an EV battery charger, isolation transformers are a must since they provide galvanic isolation between the user and the rest of the high voltage (HV) system [1]. On the AC grid or on the charger, galvanic isolation may be implemented. Grid-side isolation transformers tend to be larger than charger-side isolation transformers. [2] High frequency switching has made it possible to reduce the size of galvanic isolation transformers owing to semiconductor technological developments. Solar grid-coupled systems [3] have been employed in commercial charging infrastructure in the past. The AC grid benefits as a consequence of these technologies. Using a solar and grid-interconnected charging system for electric vehicles (EVs) at home may be advantageous. Household applications up to 10 kW may be powered by single-phase inverters [4][5]. Home solar PV may be connected to the grid in a variety of ways, including isolated and non-isolated topologies [4]- [6]. Home PV EV charging systems must have features like isolation and voltage boost capabilities in order to match the voltage of the solar PV array to grid requirements.. This topology, known as ZSI, first appeared in [7]. In a single stage, DC input voltage may be inverted, bucked, or boosted. There has been a lot of interest in photovoltaic grid-connected applications. The ZSI design makes use of two capacitors and two inductors to boost the DC input voltage to satisfy the inverter's AC output voltage specifications. The passive components of a ZSI must play a substantial role in order for it to function properly. This system may incorporate an energy storage device.

An application for a string inverter arrangement has been shown in this study using a single phase MZSI based solar grid linked charger. In part II, we looked at how a ZSI works and the components that go into

International Journal of Multidisciplinary Engineering in Current Research
ISSN NO: 2456 - 4265
Volume 5, Issue 11, November 2020, http://ijmec.com/

it. The converter is modelled and controlled in Section III, which deals with component size, modelling, and control. Simulated findings for a 3.3kW proposed inverter charger and experimental data from a proof-of-concept are presented in Section IV. Section V, the conclusion, is found here.

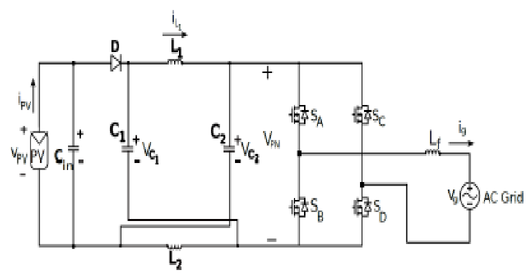

Fig. 1. Schematic of a Photovoltaic/AC grid inter-connected Z-source Inverter(ZSI)

II. TRADITIONAL ZSI

There are two modes of operation for the ZSI structure depicted in Fig.1: shoot through and non shoot through [7]. For symmetrical procedures, use

$$i_L = i_{L1} = i_{L2} \tag{1}$$

$$V_C = V_{C1} = V_{C2} \tag{2}$$

S1, S3, S2, and S4 are all on at the same time during the shoot-through condition. Longevity of this shoot through state is measured by duty cycle (D0) and switching frequency (FSW). The shoot-through condition may be achieved using a modified PWM technique described in [7]. Thus, the voltages of the two capacitors are as follows:

$$V_C = \frac{1-D_0}{1-2D_0} v_{pv} \tag{3}$$

As a result, the input voltage to the DC connection, VPN, is kept at a greater peak value. According to [7], the highest DC link voltage VPN is:

$$\hat{V_{PN}} = \frac{1}{1-2D_0} v_{pv} \tag{4}$$

The power balance equation between the DC and AC sideof the ZSI is expressed as [7],

$$(1-D_0)\hat{V_{PN}} I_{PN} = i_{grms} v_{grms} \tag{5}$$

where IPN and VP^N are the peak DC link current and voltage.The peak AC voltage of the ZSI is [7]:

$$V_g = M\hat{V_{PN}} \tag{6}$$

Where the M is the modulation index, grid voltage, vg=Vgsin! tand the grid current it=Igsin (!t+_). For _=0 for grid connectedapplications. From equation (11) and (13) the RMS ofthe output AC voltage of the ZSI is [7]:

$$V_{grms} = \frac{M v_{pv}}{\sqrt{2}(1-2D_0)} \tag{7}$$

III. COMPONENT SIZING, MODELING AND CONTROL OFPROPOSED MZSI

Fig. 2 shows a modified Z source inverter has been proposedhaving an integrated charger. The two capacitors C1 and C2from Fig.1 are split and each of them act as one of thelegs of one of the two primaries of the split primary isolatedhalf bridge converter. The MOSFET SR allows bidirectionaloperation of the MZSI when required. The diode DPV blocksthe reverse flow of current back into the PV. Rin is theinternal resistance of the input capacitor Cin. For symmetricaloperation of the MZSI, a split primary isolated DC to DCconverter has been proposed for the integration of the chargerside into the ZSI. The split primaries contain two half bridgeconverter (HBC) primaries isolated from a single full bridgesecondary through a high frequency transformer. The HBCprimaries and thesecondaries are operated at 50% duty cyclein open loop. The output current of the secondary is connectedto an energy storage unit such as a lithium-ion (Li-ion) battery.The energy storage unit clamps its own voltage, vB, acrossthe input of the HBC primaries, VC, such that,

$$V_C = 2v_B \tag{8}$$

A. Maximum Shoot Through Duty Ratio,D0max

International Journal of Multidisciplinary Engineering in Current Research
ISSN NO: 2456 - 4265
Volume 5, Issue 11, November 2020, http://ijmec.com/

As a result of the energy storage unit being connected acrossthe capacitors, the maximum shoot through duty ratio, D0maxis calculated based on the minimum input voltage, vpvmin andthe maximum battery voltage, VBmax connected across thecapacitors and is expressed as:

$$D_{0max} = \frac{2V_{Bmax} - v_{pvmin}}{4V_{Bmax} - v_{pvmin}} \quad (9)$$

SAE J1772 standard defines the standard battery voltages forDC charging between 200V-500V.

B. Inductor L1 and L2 design

The inductors L1 and L2 are sized for high frequencypeak to peak current ripple assumed between 15-25% of the

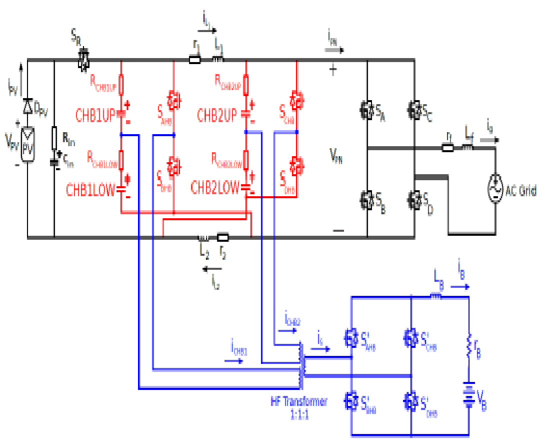

Fig. 2. Detailed Schematic of Proposed MZSI

Inductor current during the shoot-through time interval D0T/2as follow [8]:

$$L_1 = L_2 = \frac{V_{Cmax} D_{0max}}{2\Delta i_L f} \quad (10)$$

C. Capacitor C1 and C2 design

They are sized to absorb the second-order harmonic component of capacitor voltages as follows: [8]

$$C_1 = C_2 = \frac{P}{2\omega \Delta V_C V_C} \quad (11)$$

Where _VC is the specified voltage ripple limit and VC is the average voltage across the capacitors VC1 and VC2. Rad/s is the second-order harmonics represented in radians per second. Oversized electrolytic capacitors for second order harmonic suppression in single phase Z source inverters might lead to a large system. Capacitance may be reduced using a DC side Active Power Filter (APF) like the one presented in [9]. It is not reliant on the MZSI to function. There must be at least twice as much capacity in the capacitor as the energy storage device clamped across it for the suggested design.

D. Average Modeling of the Integrated Half-Bridge DCDC

Converter Charger

When an energy storage device is attached to the charger's secondary side, the charger's split primaries function alternately and provide half of the battery current needed. In the DC-DC converter, each of the converter's primary is linked to the capacitor on each leg of the converter. Capacitors are characterized by their voltage across the equation (15). In [10], the split main DC-DC converter's thorough average modelling is discussed. The simplified equivalent model of the Fig.4 shows that each of the two primaries may be represented by an RLE circuit connected parallel to each of the capacitors, C1 and

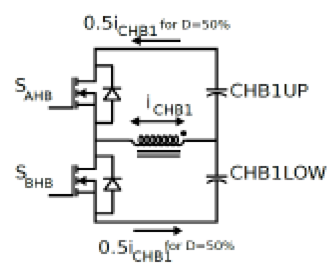

C2.

Fig. 3. Schematic of one the Primary across CHB1 operating at 50%duty cycle.

E. State Space Average Modeling of the Single Stage

Inverter ChargerThe detailed state space average modeling was presented in[10]. The equivalent diagram of the modeled MZSI is shownin the Fig. 4, during the non shoot-through state, the KVLequation is given by:

$$L\frac{di_L}{dt} = v_{pv} - i_L r + R_{HB} + (2\bar{i_g} + \frac{i_B}{2})R_{HB} - V_C \quad (12)$$

The KCL equation is:

$$C\frac{dV_C}{dt} = i_L - \bar{i_g} - \frac{i_B}{4} \quad (13)$$

During the shoot-through state, the KVL equation is:

International Journal of Multidisciplinary Engineering in Current Research
ISSN NO: 2456 - 4265
Volume 5, Issue 11, November 2020, http://ijmec.com/

$$L\frac{di_L}{dt} = V_C - i_L(R_{HB} + r) - \frac{i_B}{2}R_{HB} \qquad (14)$$

The KCL equation is written as:

$$C\frac{dV_C}{dt} = -i_L - \frac{i_B}{4} \qquad (15)$$

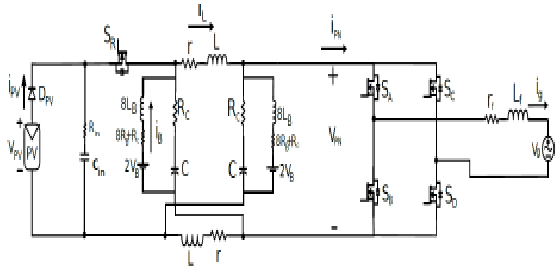

Fig. 4. Equivalent Model of the proposed Modified Z-source Inverter (MZSI) with battery

From equation (12)-(15), state space equations for theentire system can be written as:

$$\begin{bmatrix} \dot{i}_L \\ \dot{V}_C \\ \dot{i}_B \end{bmatrix} = \begin{bmatrix} -\frac{-(r+2R_{HB})}{L} & -\frac{1-2D_0}{L} & \frac{(1-2D_0)}{2}R_{HB} \\ \frac{1-2D_0}{C} & 0 & -\frac{1}{4C} \\ \frac{1-2D_0}{L_B}R_{HB} & \frac{1}{2L_B} & -\frac{R_{HB}+R_B}{2L_B} \end{bmatrix} \begin{bmatrix} i_L \\ V_C \\ i_B \end{bmatrix} + \begin{bmatrix} \frac{2(1-D_0)R_{HB}}{L} \\ -\frac{1-D_0}{C} \\ -\frac{(1-D_0)R_{HB}}{L_B} \end{bmatrix} [i_d] + \begin{bmatrix} \frac{(1-D_0)}{L} \\ 0 \\ 0 \end{bmatrix} [v_{pv}] + \begin{bmatrix} 0 \\ 0 \\ -\frac{1}{L_B} \end{bmatrix} [V_B] \qquad (16)$$

Fig. 4 shows the positive directions of the battery current,

bid and it, the grid-side AC current, respectively. The suggested MZSI topology's controller block diagram is shown in Figure 5. The PVcurrent ipv loop, the grid currentit loop, and the battery currentbid loop make up this system.

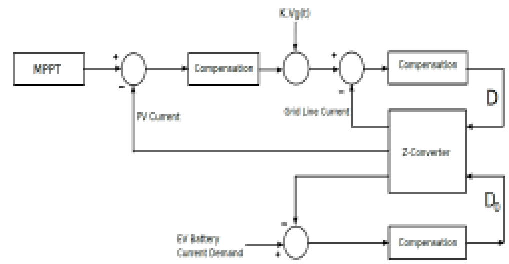

Fig. 5. Block diagram of the Control Scheme Proposed Modified Source Inverter Charger

For H-Bridge inverter output current [11] or D0 shoot-through duty ratio [12], voltage control of the ZSI capacitor is used in literature. The peak photovoltaic input current is controlled in this study to create the reference current [13]. Both capacitors will have an effect on the shoot-through duty ratio, D0, when VC is applied across them. Battery current loop control has the slowest reaction time compared to input current control since it does not need rapid dynamic changes. The transfer function is provided by the battery loop control:

$$\frac{I_B(s)}{d_0(s)} = \frac{-sC[4R_{HB}i_L - 2R_{HB}i_d] - [2i_L - i_d]}{2L_BCs^2 + sC[R_{HB} + 2R_B] + 0.25} \qquad (17)$$

A feed forward is added to the battery control loop,

$$FF_B = \frac{2V_B - v_{PV}}{4V_B - v_{PV}} \qquad (18)$$

Where VB is the output voltage of the HBC and vPV is thetracked PV voltage.The output AC side current controller should have the fastestresponse.

F. Energy Management Scheme for the Proposed Converter

The suggested system is shown schematically in Fig. 6 (below). Equation (5) is altered as follows [14] when an ESS is incorporated into a ZSI:

$$v_{PV}i_{PV} = v_b i_b + i_{grms}v_{grms} \qquad (19)$$

PB is maintained at the ESS because of the single phase AC grid power Pg, which counteracts the variability in power from the PV source Ppv. When pulling power from the grid to charge an EV battery, the direction of the AC grid current typically switched from positive to negative. The charger is powered by the PV and the grid, which may be used

International Journal of Multidisciplinary Engineering in Current Research

ISSN NO: 2456 - 4265

Volume 5, Issue 11, November 2020, http://ijmec.com/

to drive the inverter in both directions.

$$v_{PV} i_{PV} + i_{grms} v_{grms} = v_b i_b \qquad (20)$$

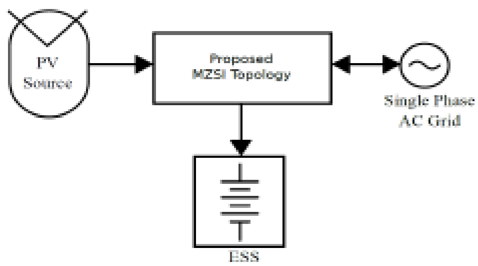

Fig. 6. Simplified Block Diagram of the System

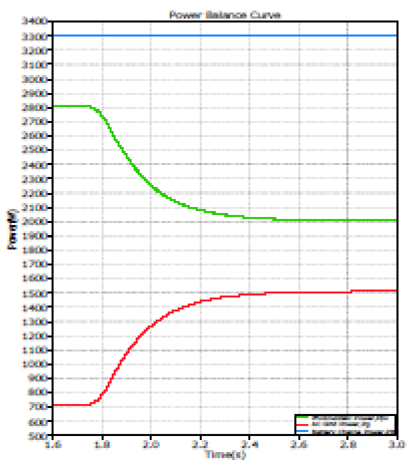

Simulated waveform for power balancing between PV, AC grid, and battery power shown in Fig. 7. Photovoltaic power, the AC grid, and battery power The MZSI may be used as a grid-connected rectifier/charger if the voltage across the input capacitor Cin is kept to at least the minimum value of the PV voltage. [15]-[16]. Previous research on ZSI topology anti-islanding protection approaches may be found in [17].

IV. SIMULATION AND EXPERIMENTAL RESULTS

A. Simulation study for a MZSI operation

The simulation studies to demonstrate the behaviour of theproposed topology have been carried out using PLECS 4 for a3.3 kW charger for a string inverter configuration. Simulationhas been carried out for the system shown in Fig.2Fig.7 shows at simulation time t=1.75 s, the input PV powerreduces from 2.8 kW to 2 kW, the grid power increases from710 W to 1500 W to maintain the output charger power to3.3kW and the corresponding grid current, DC link voltage,capacitor voltage and the battery current is shown in Fig.8.

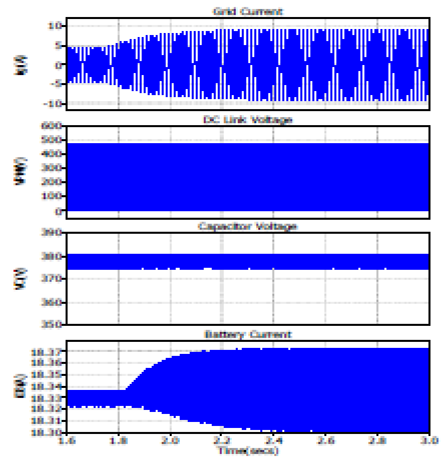

Fig. 8. Simulation Waveform of the grid current,Ig, DC link voltage,VPN,Capacitor Voltage,VC1, and Battery current,ib for the power balancebetween the Photovoltaic input power, the AC Grid side and the batterypower.

TABLE I MODIFIED ZSI BASED CHARGER SYSTEM SIMULATION SPECIFICATIONS

Parameters	Value
Input Voltage, V_{in}	286 V
Input Current, I_{in}	9.8 A
Inductor Value, L_1=L_2	500 uH
ZSI Switching Frequency, F_{SW}	25 kHz
Grid Voltage (RMS), V_g	240 V
Inverter Output Filter Inductor, L_f	7.5 mH
PV Input Power, P_{PV}	2.8 kW
Input Capacitor, C_{in}	2 mF
HBC Switching Frequency, f	50 kHz
HBC Output Filter, L_B	1 mH
Battery charge power, P_B	3.3 kW

TABLE II COMPONENT MODELS USED FOR LOSS MODELING OF THE PROPOSED SYSTEM

Component	Value
Diode, D	STTH6010W
ZSI MOSFETs [S_A, S_B, S_C and S_D]	APT28M120L
HBC MOSFETs [S_{AHB}, S_{BHB}, S_{CHB} and S_{DHB}]	APT28M120L
HBC Diodes, [S'_{AHB}, S'_{BHB}, S'_{CHB} and S'_{DHB}]	STTH6010W
Capacitor, C_{in}, C_1 and C_2	ECE-T2VP182FA

B. Loss Modeling

International Journal of Multidisciplinary Engineering in Current Research

ISSN NO: 2456 - 4265

Volume 5, Issue 11, November 2020, http://ijmec.com/

The loss modeling for the proposed system shown in Fig.2 has been carried out by modeling the actual components inPLECS 4.0. The switching components used for the modelingis shown in the Table II,For the loss modeling of the passive components, theinternal resistance of the inductors, L1, L2 and Lf are r=100m and the ESR, RHB for the capacitors C1, C2 and Cin

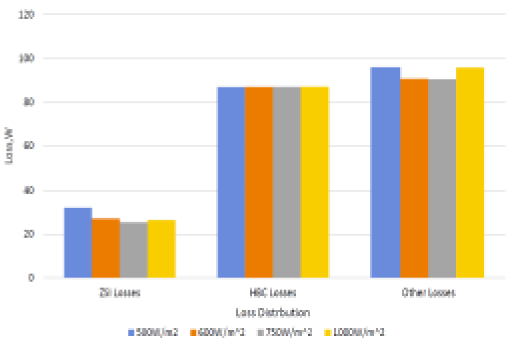

Fig. 9. Loss distribution chart for the MZSI topology for a fixed chargingpower PB=3.3 kW at 25 _C, under varying irradiation

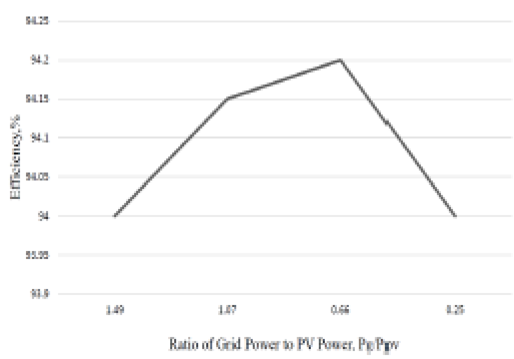

Fig. 10. Efficiency curve for different ratios of AC Grid Power Pg toPhotovoltaic Power Ppv curve for a fixed charging power PB=3.3 kW at25 _C under varying irradiationare 138 m.

Fig. 9 shows the loss distribution between the ZSI (conductionand switching losses of the MOSFETs and diode D), theHBC (conduction and switching losses of the MOSFETs andsecondary diodes) and other losses in due to the inductor, capacitors,leakage losses in the high frequency transformer andbattery series resistances in the system for varying irradiationsfor a constant charging power PB=3.3 kW.Fig. 10 shows the efficiency is around 94% from theefficiency curve for various ratios of AC Grid Power,Pg, toPhotovoltaic Power, Ppv for a fixed charging power, PB=3.3kW at 25 _C, for varying irradiation between 500W=m2to 1000W=m2. Although the efficiency variations is small,the efficiency is the highest when the sharing between thephotovoltaic power Ppv and the grid power Pg is equal.For a constant frequency of operation, the HBC MOSFETlosses remain constant for a fixed value VB and chargingpower, PB. Although in reality, this might not be the case. The efficiency of the converter will change with the change inthe battery voltage. Fig. 11 shows the distribution of the lossesbetween the ZSI losses, the HBC MOSFETs and the losses due

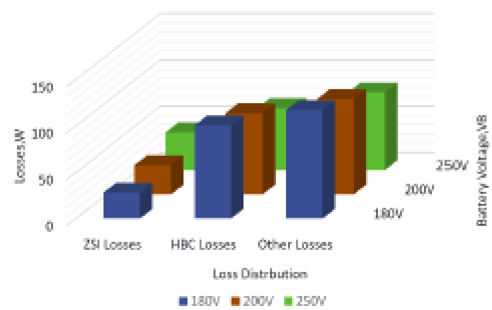

Fig. 11. Loss distribution for various battery voltages,VB, for a fixedcharging power,PB=3.3 kW, at 45 _C

TABLE IIIMODIFIED ZSI BASED CHARGER SYSTEM PROTOTYPE ELECTRICALSPECIFICATIONS

Parameters	Value
Input Voltage, V_{in}	38 V
Input Current, I_{in}	3.82 A
Inductor Value, L_1 & L_2	500 uH
Peak DC Link Voltage, V_{PN}	63.33 V
Modulation Index, M	0.75
Shoot Through Duty Ratio, D_{0MAX}	0.2
Switching Frequency, F_{SW}	25 kHz
Grid Voltage, V_g	34 V(RMS)
Inverter Output Filter Inductor, L_f	2.5 mH
HBC switching frequency, f_{HBC}	50 kHz

Transformer and battery series resistances in the system forvarious battery voltages. From Fig.11,at 45 _C, the vpv dropsto 258V and it can be observed that

International Journal of Multidisciplinary Engineering in Current Research
ISSN NO: 2456 - 4265
Volume 5, Issue 11, November 2020, http://ijmec.com/

with the increase in batteryvoltage the ZSI losses increase but the HBC losses and thelosses in the passive components reduce.

C. Experimental Verification of the MZSI power balanceoperation

In this paper as proof of concept, a scaled down 175Wexperimental setup was built using MATLAB/Simulink andspace 1103.The setup has the following specificationsshown in table III.Fig. 12 shows the PWM scheme for the HBC. Each ofthe split primary operate for half the HBC switching period.Each MOSFET SAHB, SBHB, SCHB and SDHB operatesexclusively for one quarter of the entire HBC switching period.Equation (23) can be written in terms of the current sharingbetween the AC load (grid) and the battery as:

$$i_{PV} = \frac{1-D_0}{2(1-2D_0)} i_b + \frac{M}{\sqrt{2}(1-2D_0)} i_g \qquad (21)$$

Where M is the modulation index and D0 is the shoot throughduty ratio. For D0=0.2,

$$i_{PV} = \frac{2}{3} i_b + \frac{\sqrt{3}}{2} i_g \qquad (22)$$

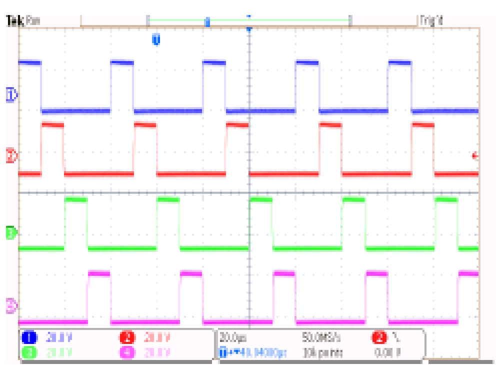

Fig. 12. PWM logic for the isolated HBC

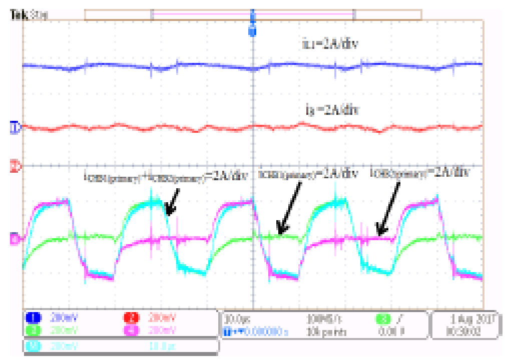

Fig. 13. Experimental setup waveforms for the Inductor current (top),charger output current (middle) and the primary currents of the splitcharger (bottom)

From equation (22), at D0=0.2, for an input current up =3.82A and fixed HBC output current if=2 A, the ZSI AC outputcurrent it is calculated to be 2.87 A.Fig.13 shows the inductor current iL1, the battery currentbid and the split primary current iCHB1 and iCHB2 and thetotal primary current. Each of the primary operate alternately.The total primary current is a high frequency alternatingcurrent of fob=50 kHz.From Fig. 13 and Fig. 14, the charger output current ismaintained at 2 A using a Chroma Programmable AC/DC ElectronicsLoad (Model 6304). The PV input current is maintainedat 3.82 A using a Magna-power LXITM solar emulator.The output grid current is observed to be 2.66 A. Fig. 15 showsthe experimental setup for the proof of concept.The lower values of the output current is a result of thelosses in the circuit. The practical PI values for the Aside current control was KP =0.03 and the battery loop wasKPB=.0003 and KIB=.09 and the input PV current loop werePin=0.005 and Kirin=2.

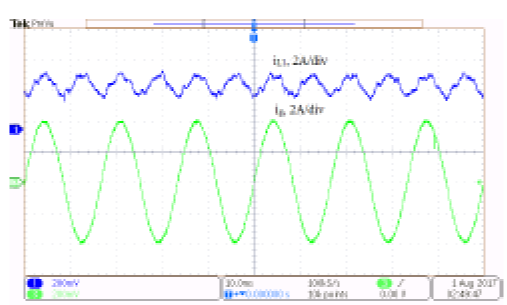

International Journal of Multidisciplinary Engineering in Current Research

ISSN NO: 2456 - 4265

Volume 5, Issue 11, November 2020, http://ijmec.com/

Fig. 14. Experimental waveform input current (blue) and output current (green) between the charger and the AC output of the MZSI

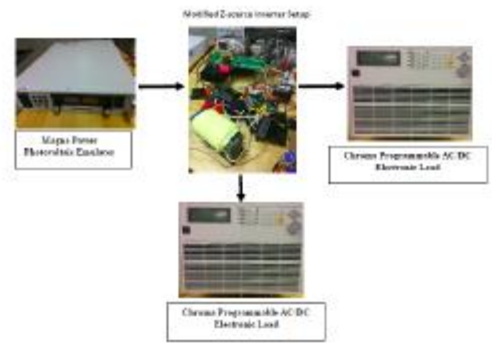

Fig. 15. Experimental setup

Table IVIsolated Half Bridge Dc-Dc System ElectricalSpecifications

Parameters	Value
Input Voltage, V_C	50.667 V
Output Voltage , V_B	25.335 V
Switching Frequency, $F_{sw(H B}$	50 kHz
Filter inductor, L_B,	330 uH

V. CONCLUSION

A modified ZSI architecture has been described in this research provides an intriguing option for solar grid linked charging systems. It comprised of a single stage photovoltaic grid (PV-Grid) connection and an integrated charger for PV-Grid linked charging or energy storage. This topology may be used to centralized setup for charging in semi-commercial places such as a parking lot of a shopping mall. For residential applications, this notion may be expanded to string inverters with the charger side of the string inverter configurations coupled in series or parallel for current sharing. The research presents a new energy storage design employing Z source converter through\symmetrical functioning of its impedance network.

REFERENCES

[1] D. Agiler, F. Canales, H. Belaya, D. L. Parra, A. Cocoa,N. Butcher, and O. Apeldoorn, "Ultra-fast dc-chargeinfrastructures for eve-mobility and future smart grids," inProc. of IEEE PES Innovative Smart Grid TechnologiesConference Europe, pp. 1–8, Oct. 2010.

[2] G. Carli and S. S. Williamson, "Technical considerationson power conversion for electric and plug-in hybridelectric vehicle battery charging in photovoltaic installations,"IEEE Trans. on Ind. Electron., vol. 28, no. 12,pp. 5784–5792, 2013.

[3] J. G. Ingersoll and C. A. Perkins, "The 2.1 kw photovoltaicelectric vehicle charging station in the city ofSantaMonica, California," in Proc. of the Twenty FifthIEEE Photovoltaic Specialists Conference, pp. 1509–1512, May. 1996.

[4] S. B. Kaur, J. K. Pedersen, and F. Bleiberg, "A reviewof single-phase grid-connected inverters for photovoltaicmodules," IEEE Trans. on Ind. Appl., vol. 41, no. 5, pp.1292–1306, Sep. 2005.

[5] N. A. Nina, L. A. C. Lopes, and I. S. Member, "Operationof Single-phase Grid-Connected Inverters with LargeDC Bus Voltage Ripple," Proc. of the IEEE CanadaElectrical Power Conference, 2007.

[6] S. Bay, D. Yu, and S. Ludic, "Optimum design of aneve/phi charging station with dc bus and storage system,"in Proc. of IEEE ECCE, pp. 1178–1184, Sep. 2010.

[7] F. Z. Pang, "Z-Source Inverter," in IEEE Trans. on Ind.Appl., vol. 39, no. 2, pp. 504–510, 2003.

[8] Y. Huang, M. Sheen, F. Z. Pang, and J. Wang, "Sourceinverter for residential photovoltaic systems,"IEEE Trans. on Power Electron., vol. 21, no. 6, pp. 1776–1782, Nov. 2006.

[9] S. A. Singh, N. A. Aziz, and S. S. Williamson, "Capacitancereduction in a single phase quasi z-source inverter

Using a hysteresis current controlled active power filter, "in in Proc. of IEEE 25th Int. Symptom Ind. Electron., pp.805–810, Jun. 2016.

[10] S. A. Singh, G. Carli, N. A. Aziz, and S. S. Williamson,"A modified z-source converter based single phasepave/grid inter-connected dc charging converter for futuretransportation electrification," in Proc. of IEEE ECCE,pp. 1–6, Sep. 2016.

[11] Y. Li, S. Jiang, J. G. Cintron-Rivera, and F. Z. Pang,"Modeling and control of quasi-z-source inverter fordistributed generation applications," IEEE Trans. on Ind.Electron., vol. 60, no. 4, pp. 1532–1541, Apr. 2013.

International Journal of Multidisciplinary Engineering in Current Research
ISSN NO: 2456 - 4265
Volume 5, Issue 11, November 2020, http://ijmec.com/

[12] T. Chandrasekhar and M. Veer chary, “Control ofsingle-phase z-source inverter for a grid connected system,”in Proc. of Int. Conf. on Power Syst., pp. 1–6, Dec.2009.

[13] B. Gee, Y. Liu, H. Abu-Rub, R. S. Blog, F. Z. Pangs. McConnell, and X. Li, “Current ripple damping controlto minimize impedance network for single-phasequasi-z source inverter system,” IEEE Trans. on Ind.Info., vol. 12, no. 3, pp. 1043–1054, Jun. 2016.

[14] B. Gee, H. Abu-Rub, F. Z. Pang, Q. Lei, A. T. de Almeida,F. J. T. E. Ferreira, D. Sun, and Y. Liu, “An energy-storedquasi-z-source inverter for application to photovoltaicpower system,” IEEE Trans. on Ind. Electron., vol. 60,no. 10, pp. 4468–4481, Oct. 2013.

[15] J. Rabkowski, R. Barlik, and M. Nowak, “Pulse widthmodulation methods for bidirectional/high-performancez-source inverter,” in Proc. of IEEE Power Electron.Spec. Conf., pp. 2750–2756, Jun. 2008.

[16] S. Dong, Q. Zhang, and S. Cheng, “Analysis of criticalinductance and capacitor voltage ripple for a bidirectionalz -source inverter,” IEEE Trans. on Power Electron.,vol. 30, no. 7, pp. 4009–4015, Jul. 2015.

[17] M. Trabelsi and H. Abu-Rub, “A unique active antiislandingprotection for a quasi-z-source based powerconditioning system,” in Proc. of IEEE Appl. PowerElectron. Conf.e and Expo., pp. 2237–2243, Mar. 2015